The relativistic electron response at geosynchronous orbit during the January 1997 magnetic storm

G. D. Reeves,[1,2] R. H. W. Friedel,[1,2] R. D. Belian,[1] M. M. Meier,[1] M. G. Henderson[1],
T. Onsager,[3] H. J. Singer,[3] D. N. Baker,[4] X. Li,[4] and J. B. Blake[5]

Abstract. The first geomagnetic storm of 1997 began on January 10. It is of particular interest because it was exceptionally well observed by the full complement of International Solar Terrestrial Physics (ISTP) satellites and because of its possible association with the catastrophic failure of the Telstar 401 telecommunications satellite. Here we report on the energetic electron environment observed by five geosynchronous satellites. In part one of this paper we examine the magnetospheric response to the magnetic cloud. The interval of southward IMF drove strong substorm activity while the interval of northward IMF and high solar wind density strongly compressed the magnetosphere. At energies above a few hundred keV, two distinct electron enhancements were observed at geosynchronous orbit. The first enhancement began and ended suddenly, lasted for approximately 1 day, and is associated with the strong compression of the magnetosphere. The second enhancement showed a more characteristic time delay, peaking on January 15. Both enhancements may be due to transport of electrons from the same initial acceleration event at a location inside geosynchronous orbit but the first enhancement was due to a temporary, quasi-adiabatic transport associated with the compression of the magnetosphere while the second enhancement was due to slower diffusive processes. In the second part of the paper we compare the relativistic electron fluxes measured simultaneously at different local times. We find that the >2-MeV electron fluxes increased first at noon followed by dusk and then dawn and that there can be difference of two orders of magnitude in the fluxes observed at different local times. Finally, we discuss the development of data-driven models of the relativistic electron belts for space weather applications. By interpolating fluxes between satellites we produced a model that gives the >2-MeV electron fluxes at all local times as a function of universal time. In a first application of this model we show that, at least in this case, magnetopause shadowing does not contribute noticeably to relativistic electron dropouts.

1. Introduction

On January 6 and 7, 1997, a "halo" coronal mass ejection (CME) was observed by the SOHO Large Angle and Spectrometric Coronograph. Its appearance suggested that it was directed toward the Earth, roughly along the line of sight. The CME was observed in the solar wind by both the SOHO and Wind spacecraft which were located at approximately X=230 R_E and X=85 R_E respectively. As the CME passed by the satellites it was quickly recognizable as a 'magnetic cloud' event [e.g., *Bothmer and Schwenn*, 1995]. (Key parameter data from Wind, courtesy of K. Ogilvie and R. Lepping, are shown in Figure 1.) The leading half of the magnetic cloud contained southward interplanetary magnetic field (IMF) B_Z which produced strong substorm activity in the magnetosphere (as will be shown below). The trailing half contained strong northward field but additionally was accompanied by a large density enhancement that strongly compressed the magnetosphere.

The event has caused considerable scientific interest because it was exceptionally well observed by the ground- and satellite-based network that makes up the International Solar Terrestrial Physics (ISTP) program [*Acuna et al.*, 1995]. A major goal of the ISTP program is to combine measurements from multiple spacecraft in order to develop a more comprehensive picture of the response of the magnetosphere to solar wind conditions. The event also generated significant public interest because of its association with the catastrophic failure of the Telstar 401 satellite, which affected communications and broadcast capabilities and alerted the public and policy-makers to the susceptibility of sophisticated satellite-based systems to the effects of the space environment [*The Washington Post*, January 23, 1997, p. 1]. As a result of this interest a large number of studies, workshops, and special sessions are in progress or have been arranged. This paper describes the magnetospheric energetic electron response at geosynchronous orbit. We examine the substorm responses and the two-phase relativistic electron enhancement. In addition, we analyze the response as a function of local time and present a model synthesis that provides a global picture of the geosynchronous relativistic electron environment.

2. Magnetospheric Response to IMF Conditions

2.1. Substorm Response During Southward IMF

Figure 1 provides an overview of the magnetospheric response to the passage of the magnetic cloud over the interval from January 9 to 12, 1997. The top three panels show data from the Los Alamos energetic electron detectors on satellites 1990-095, 1991-080, and 1994-084. The fourth panel shows the B_Z (in GSM coordinates) and total magnetic field strength measured by GOES 9. GOES 8 had an unusual and unfortunate loss of data from the middle of January 9 to the end of January 10. (Table 1 gives the locations of all five geosynchronous satellites.) Panels five and six show the IMF B_Z and solar wind ion density measured by Wind, and panel seven shows the preliminary *Dst* index (courtesy of WDC/Kyoto) and the pressure-corrected *Dst** (courtesy of G. Lu).

The geosynchronous particles and fields show that the magnetosphere was relatively quiet on January 9, a reflection of the relatively weak IMF B_Z values. After fluctuating at values near zero the IMF B_Z at Wind turned suddenly northward at approximately 0053 UT on January 10 in association with the passage of a shock front. The effect of the shock on the magnetosphere was observed about 10 min later as a weak enhancement of the GOES 9 magnetic field strength and 1994-084 energetic electron fluxes. At 0204 UT the IMF B_Z turned southward and stayed southward for about 45 min, initiating moderate substorm activity in the magnetosphere. Thereafter the IMF B_Z showed large-amplitude fluctuations until 0442 UT, when it again turned sharply southward. It then remained southward for over 12 hours, reaching peak values of -15 nT.

During the period of strong, steady southward IMF the magnetospheric response was characteristic of geomagnetic storms. The geosynchronous energetic particles showed large and rapid fluctuations indicative of the strong fluctuations in the magnetic and electric fields. The fluctuations in both the particles and fields are particularly pronounced when the observing spacecraft is near midnight local time, but fluctuations are observed at all local times. We emphasize that large and rapid fluctuations of the energetic particle fluxes, rather than exceptionally high flux levels, are the feature that characterizes storm times. In fact, individual substorms within the storm period are nearly impossible to identify. Nevertheless, many particle injections and dipolarizations of the magnetic field are apparent, and traditional substorm indicators do show high levels of activity. The peak value of the *Kp* index (courtesy of NOAA/SEC) on January 10 was 6, and peak values of the preliminary *AE* index (courtesy of WDC/Kyoto) reached 2000. *Baker et al.* [1998*a*] have estimated the "geoeffectiveness" of the January 1997 storm and calculated that the magnetospheric "coupling parameter," epsilon, reached values around 10^{12} W and stayed well above 10^{11} W for most of the cloud interval.

2.2. Magnetospheric Compression During Northward IMF

After a nearly linear increase the IMF B_Z became slightly northward at 1734 UT but soon dropped to slightly negative values before becoming firmly northward at 2046 UT. The northward turning of the IMF led to an abrupt cessation of substorm activity. The energetic electron fluxes at satellite 1994-084 showed a final injection at 1853 UT, and no further substorm activity was visible until nearly 1200 UT on January 11 after the IMF had again been slightly southward. At that time, satellite 1994-084 observed a strong growth phase dropout followed by a small substorm injection and increase in *AE* to above 500.

Although there were no substorms during the passage of northward IMF, the magnetosphere was far from quiet. As Figure 1 shows, the IMF was strongly northward for most of the period from 2046 UT on January 10 to 0800 UT on January 11. As the IMF turned northward, the solar wind ion density began to increase. Then at 0053 UT it increased suddenly by about a factor of 3, peaked at nearly 200 cm^{-3}, and then decreased suddenly at about 0201 UT. At 0116 UT the compression of the magnetopause was felt at geosynchronous orbit. The GOES 9 magnetic field data show a strong compression of the field, and at the same time, spacecraft 1991-080 and 1994-084 saw a sudden change in the spectrum with lower-energy channels showing a step up in flux and higher-energy channels showing a step down, indicating that the satellites suddenly found themselves on new "*L* shells" with a softer energetic electron spectrum. The *Dst* index also shows the effects of the solar wind density enhancement and even became positive for several hours at the beginning of January 10, while the pressure corrected *Dst** showed the more traditional gradual storm recovery with no positive excursions. All these signatures are typical of a magnetospheric compression.

A complete dropout of energetic particles was observed by spacecraft 1994-084 from 0154 to 0217 UT and again from 0312 to 0316 UT. Data from the magnetospheric plasma analyzer (MPA) instrument, which measures plasmas with energies below 40 keV, confirms that during these intervals 1994-084 crossed the magnetopause and entered the magnetosheath (*M. F. Thomsen, personal communication*, 1997). The local times of 1994-084 during these two magnetopause crossings were approximately 1000 LT and 1100 LT respectively. Spacecraft 1991-080, located approximately 2 hours earlier in local time, also observed an energetic particle dropout for about 1 min at 0212 UT, but this dropout was not complete, so the spacecraft approached but did not cross the magnetopause. Most magnetopause crossings at geosynchronous orbit are produced by a combination of strong pressure enhancements and strong southward IMF that erodes the magnetopause through reconnection. Therefore this crossing, for which the IMF was strongly northward, was somewhat unusual and noteworthy.

2.3. Relativistic Electron Response

An enhancement of electrons with energies above 1 MeV is frequently observed following geomagnetic storms; however, the precise acceleration mechanism is not yet known. *Blake et al.* [1997] have shown that a combination of strong southward IMF and high solar wind velocity can produce relativistic electron enhancements that typically peak several days after the initial onset of geomagnetic activity [e.g. *Baker et al.*, 1998*b*]. In the January 1997 storm there was certainly strong southward IMF, which drove substorm injections that may be the "seed population" for further acceleration to relativistic energies. The solar wind velocity during the cloud was in the range of 400-475 km/s, but following the passage of the cloud, values approaching 600 km/s were observed. While this velocity is not as high as that in some of the coronal hole produced enhancements observed near solar minimum, it appears to have been sufficient.

Figure 2 shows 1-min and 1-hour averages of the electron fluxes from selected energy channels (50 keV to 6 MeV) from the synchronous orbit particle analyzer (SOPA) [*Belian et al.*, 1992] and energetic spectrometer for particles (ESP) [*Meier et al.*, 1996] instruments on spacecraft 1991-080. A diurnal variation due to the spacecraft orbit is apparent in all energies. Peak fluxes tend to be observed near local noon (0718 UT for 1991-080) when, as a result of magnetic asymmetries, the satellite tends to be on slightly lower *L* shells. However, at lower energies (e.g., approximately 50-500 keV), substorm injections can produce additional flux enhancements with maximum intensities observed near local midnight.

In addition to the diurnal variations the response to the passage of the magnetic cloud can also be observed. In Figure 2a we have

plotted 1-min data from January 9 to 12 when the magnetic cloud was passing the Earth, and in Figure 2b we show the expanded period from January 8 to 18. When the southward IMF begins to produce strong injections at energies below about 300 keV, the electrons at energies above about 1 MeV actually show a decrease. (The 3.5 to 6.0 MeV channel is at cosmic ray background levels and therefore shows no decrease.) The first increase of relativistic electrons began around 1200 UT on January 10, but at this time the fluxes are still strongly modulated by magnetic field fluctuations. A much more pronounced increase began around 1900 UT in close association with the final substorm injection noted above. The relativistic electron fluxes remained high until about 1200 UT on January 11 — which is the approximate time of the failure of the Telstar 401 satellite.

Enhancements of relativistic electrons are known to cause spacecraft anomalies through deep dielectric charging in insulators such as those in power systems and cables and the subsequent discharges that can cause logic errors and physical damage in electronic systems [e.g., *Wrenn*, 1995; *Baker et al.*, 1996]. Therefore the timing of the Telstar failure is suggestive. However, as Figure 2c illustrates, the conditions during January 10-11, 1997 were not extreme.

Figure 2c shows 1-hour averages of data for days 3 to 50 of 1997. Three distinct periods of relativistic electron enhancements can be observed and are shaded in the figure. One can see that the intensity of the low-energy injection activity, the levels of relativistic electron fluxes, and the spectral hardness during January 10-11 were all lower than the were at other times during these 50 days – times for which serious satellite anomalies were not reported.

What is more unusual for the January storm is the two-phase response of the relativistic electrons at geosynchronous orbit, which is apparent in Figures 2b and 2c. After the initial enhancement on January 10 and 11 the relativistic electron fluxes decreased rapidly by nearly an order of magnitude over a large range of energies. Subsequently, the fluxes again climbed to relatively high values, but this time over a period of several days, not peaking until January 15. This second, slower increase of the relativistic electron fluxes is more typical of events reported previously [e.g., *Paulikas and Blake*, 1979].

The two-phase enhancement of relativistic electrons at geosynchronous orbit may be due to two different transport processes. The first enhancement on January 10-11 appears to be associated with the compression of the magnetosphere. The second, slower enhancement, which peaked on January 15, appears to be more typical and occurred after the passage of the cloud when the solar wind was no longer driving the magnetosphere in any unusual way. Both enhancements may be the result of outward transport from a source region in the outer electron belt but inside geosynchronous orbit. A possible scenario will be discussed in the summary section.

3. Multi-Satellite Analysis

3.1. General Variations in Local Time

With five geosynchronous satellites it is possible to combine the data to provide nearly complete coverage at a variety of different local times simultaneously. This not only allows us to remove some of the diurnal variation (as seen in Figure 2) but also to examine in more detail the asymmetries in the particles and in the magnetic field that are present during the disturbance. Plate 1 shows data from the five geosynchronous spacecraft listed in Table 1. The fluxes have been normalized, somewhat arbitrarily, by quadratic fitting of the peak values observed by each satellite when it was at local noon and then normalizing those fits to the fit for spacecraft 1991-080. This procedure required multiplying (or dividing) the fluxes by the amounts indicated on the figure (approximately 1.2 or 1.7). We note that the Los Alamos National Laboratory (LANL) data cover energies nominally between 1.8 and 6 MeV, while GOES measures energies above 2 MeV. However, our simple normalization procedure is sufficient provided the spectral slope above 2 MeV does not change dramatically, and we see from Figure 2 that it does not. Additionally, we note that the GOES 8 and 9 satellites are spin-stabilized and measure primarily 90° pitch angle particles, while the LANL SOPA and ESP measurements are spin-averaged and cover essentially all pitch angles.

After normalization we can combine the data from all five satellites into a single data set. We have done so in Plate 2. Each of the four plots in Plate 2 shows the fluxes measured in each of four local time sectors. Each of the four local time sectors is 4 hours wide spanning the ±2 hours around dusk, dawn, noon, and midnight. Data from each of the five satellites are color coded. Using the data from the dusk sector, we have traced out a dashed reference line so that the fluxes can be more easily compared.

Using the dashed reference line, we can see that, on average, the fluxes at dawn and dusk are approximately equal, while the fluxes at noon consistently lie above the reference curve, and the fluxes at midnight usually lie below the reference curve. This trend is consistent with the diurnal variation that is also observed by a single satellite. The magnetic field tends to be stretched and "tail-like" at midnight but compressed and "dipole-like" at noon. This causes equatorially trapped particles to move outward at noon and inward at midnight relative to their drift trajectories in a dipole magnetic field. Because of the typically strong inward radial gradient in the fluxes this effect will produce higher fluxes at noon and lower fluxes at midnight. In addition, a satellite that is even slightly off the magnetic equator will tend to be on higher L shells at midnight than at noon and therefore will also be connected to a region of lower fluxes. The magnitude of these two effects will depend on the pitch angle distribution of the fluxes, on the strength of the radial gradient, and on a satellite's position, i.e., magnetic latitude and radial distance.

Looking at the plot for noon, we see that the normalization procedure we used does a reasonable job in that no one satellite is consistently lower than the others. We also see that there is less variation in the fluxes than at other local times. This is likely because the field is more dipole-like and has less variation than it does at other local times. Notice that in the dusk plot the data for each satellite appear to trend downward for each pass of the satellite through that local time while at dawn they appear to trend upward. This effect is due to the motion of the satellites, which is always east and therefore moves the satellites from the higher dayside fluxes to the lower nightside fluxes as it moves from 1600 to 2000 LT. From 0400 to 0800 LT the opposite happens, and the fluxes appear to increase. At midnight the

largest variations are observed. Not only do the fluxes on a given satellite vary as a result of changing configuration of the magnetic field, but there also appear to be some systematic differences between the satellites, probably because satellites on the geographic equator, but at different longitudes, are at different magnetic latitudes and therefore observe different fluxes. Because the magnetic field is most stretched on the nightside of the Earth, the differences are largest there.

An important implication for radiation belt modeling and for space weather applications is that two or more satellites at geosynchronous orbit cannot be assumed to be on the same "drift shell," especially during highly disturbed intervals. The differences in the fluxes observed by two or more satellites are also generally much larger than can be accounted for by magnetic field models, which, by necessity, tend to represent the "average" field rather than extreme conditions.

3.2. January 10 and 11

The degree to which the fluxes measured at different local times disagree depends on the degree of asymmetry in the distortion of the magnetosphere. The dashed curve showing the trend of the data in Plate 2 does a reasonable job after the middle of January 11, when the fluxes are changing slowly, but is insufficient to characterize local time differences in the initial enhancement on January 10-11. Plate 3 shows an expanded plot for January 10-12 in a more revealing format. Here we have color coded the curves according to the local time of the measurement, without regard to which satellite was taking the measurement. Another difference is that we have binned the data into local time sectors that are only 2 hours wide, extending ±1 hour on either side of dawn, dusk, noon, and midnight.

First we consider the initial enhancement of the fluxes. The fluxes of >2-MeV electrons increase by nearly a factor of 100 beginning at about 1200 UT on January 10. It is interesting that there is nothing particularly notable in the solar wind that can be associated with this sudden change. GOES 9 observed a distinct change in the magnetic field at about 1000 UT on January 10 as a result of substorm activity near midnight. Although that may be related to the relativistic electron increase seen at noon, we will see that the fluxes of relativistic electrons at dawn and dusk were not yet enhanced by that activity.

The initial increase is clearly seen at three different local times in Plate 3. At decimal day 10.57 (≈1400 UT) the fluxes at noon (gray squares) are nearly 10^3 $[cm^2/s/sr]^{-1}$, while fluxes at dusk (blue dots) are $2\text{-}3 \times 10^1$ $[cm^2/s/sr]^{-1}$. This difference is not a consequence of motion of the satellite through dusk since the fluxes are increasing rather than decreasing (as they would tend to do for a satellite moving toward midnight). The fluxes at noon may have increased earlier than those shown in Plate 4 but then there was no satellite in the local time range 1100-1300 LT. However, it is clear that the fluxes at noon increased earlier than the fluxes at dusk. Likewise the fluxes at dusk (blue dots) increased sooner than the fluxes at dawn (red dots). While these differences might be interpreted as a propagation in local time, it is more likely that they represent strong asymmetries in the magnetic field (and therefore the local electron population) at the different local times. In particular, Figure 1 shows that the initial relativistic electron enhancement occurred while spacecraft 1994-084 and 1991-080 (located near dusk) were observing large variations in energetic particle fluxes at all energies due to the highly stretched, tail-like field at those local times.

Plate 3 shows that equally large differences between the fluxes measured at different local times could be observed throughout the enhancement. Just after day 10.75 (1800 UT) a strong stretching of the magnetic field on the nightside (green squares) caused the fluxes there to decrease by about 2 orders of magnitude in comparison with the fluxes at dusk (blue), while a few minutes later the fluxes at the two local times were essentially equal. Somewhat surprisingly, such large variations are by no means confined to midnight. At day 11.1 (0230 UT) the fluxes measured simultaneously at dusk and dawn were different by nearly 2 orders of magnitude, while the fluxes on the nightside lay between the two extremes. The reversed situation was observed at day 11.5 (1200 UT), when it was the duskside fluxes that dropped out while the dawnside fluxes remained high.

3.3. A Data-Based Synthesis Model

A goal of magnetospheric physics – and particularly of the National Space Weather Program [*Office of the Federal Coordinator for Meteorology*, 1997] – is to develop magnetospheric models that provide reliable and accurate predictions of the spacecraft environment. Naturally, considerable attention has been focused on geosynchronous orbit, where the largest number of satellites operate. Given the large variations in the relativistic electron fluxes demonstrated in the preceding two sections, it is fair to ask: Are even five satellites sufficient to characterize the geosynchronous relativistic electron fluxes?

Since a single satellite can only measure the in situ fluxes, constructing a data-driven model of the relativistic electron belts requires interpolation and/or extrapolation in space. If, as in this study, we limit the coverage to geosynchronous orbit, it is sufficient to interpolate in local time or in longitude. In Plate 4 we have taken 15-min averages of the >2-MeV electron fluxes shown in Plate 1. For each local time we calculate the expected flux based on a linear interpolation between the fluxes measured by the two spacecraft on either side. This relatively simple procedure allows us to construct a complete, time-evolving picture of the relativistic electron fluxes at geosynchronous orbit.

In Plate 4 we plot the results. The format is flux (color-coded) as a function of local time and universal time. The satellite orbits (which are straight lines for geosynchronous satellites; see Table 1) are also shown. The flux values along the satellite tracks are exact, while the fluxes between satellites are interpolated values. The local time versus universal time plot format provides an "orthogonal" view to the *L* shell versus universal time plots that can be constructed from polar and elliptically orbiting satellites [e.g., *Baker et al.*, 1994; *Friedel and Korth*, 1995]. A notable difference, though, is that the geosynchronous synthesis model can resolve flux changes that occur as rapidly as a few minutes, while the temporal resolution of the *L* shell versus universal time plots is one-half orbit, which is typically 45 min at low-Earth orbit and 5-6 hours for geosynchronous transfer orbits (such as CRRES).

Naturally, many of the features that show up in the line plots shown above also appear in Plate 4. Prior to 1200 UT on January 10 the fluxes were too low to allow reliable cross calibration of the different satellites, so Plate 4 begins at that

time and runs through January 11. The initial enhancement of fluxes near noon, as compared with dusk and dawn, can clearly be seen. In fact, not until after 1400 UT on January 11, after the passage of the cloud, do the fluxes become reasonably uniform in local time. Throughout the passage of the cloud the location of the peak relativistic fluxes moves around considerably. While our determination of the exact location of the flux peak is limited by the number of satellites (and hence spatial coverage), prenoon and postnoon asymmetries are readily apparent. This feature, as we noted earlier, reflects asymmetric changes in the configuration of the dayside magnetic field, which distort the drift shells and flux boundaries rather than localized "injections" on a particular drift shell.

The highest fluxes were measured between about 1930 UT on January 10 and 0120 UT on January 11. Both Plates 1 and 4 show that those peak flux values were measured by GOES 9. Unfortunately, this time also corresponds to the period with the least coverage, since neither GOES 8 nor 1990-095 was providing data. Therefore the local time extent of this maximum is certainly exaggerated in Plate 4. Even so, it is apparent that Telstar 401 (which was located between GOES 8 and 9, several hours ahead of GOES 9 in local time) was in a location that exposed it to almost the highest levels of >2-MeV electrons that were observed in this event.

Equally notable are the "holes" that appear when one satellite observes particularly low fluxes as a result of localized magnetic field stretching. For example, the dark blue patch in Plate 4 at about 0200 LT and 2200 UT on January 10 is produced by a nightside dropout observed by a single satellite, 1991-080. Spacecraft 1994-084, which was only 2 hours away, did not measure a dropout. Likewise at approximately 1200 UT on January 11 one can see the somewhat broader dropout at 1900 LT, near dusk.

Perhaps the most interesting of the "holes" in Plate 4 is the dark blue patch observed near dawn at about 0200 UT on January 11. This hole is caused by the magnetopause compression discussed above (Figure 1). Because spacecraft 1994-084 and 1991-080 both skimmed the magnetopause, the 0200 UT hole appears fairly broad. Close examination shows that for that 15-min period the fluxes at all local times were somewhat diminished. However, it is important to note that the fluxes at other local times did not drop out completely. In particular, the fluxes at noon and dusk remained at fairly high levels, an indication that the electrons measured at geosynchronous orbit at those local times could drift there unimpeded. In particular, they were not lost on open drift orbits, – a process that has been called "magnetopause shadowing." Magnetopause shadowing has been suggested as one possible mechanism for the sudden, global dropouts of relativistic electrons that are often observed in the main phase of storms [e.g., *Li et al*., 1997]. These results show that, at least in this case, magnetopause compression does not produce a drift shadow at other local times.

The precise extent and location of holes or peaks in the fluxes at various local times cannot be calculated without a more dense array of in situ measurements. The effects of adding or removing a satellite can clearly be seen when there are gaps in the data from one or more satellites. At 0000 UT on January 11 after a gap in both GOES 8 and 1990-095 data the change was dramatic, while the gap in 1990-095 data around 1600 UT on January 11 made very little difference to the model. This finding suggests that there are times when our simple linear interpolation is a good approximation even over a large range of local times but that there are also times when it is not. Since distortions in the magnetic drift shells are caused by magnetospheric current systems, the separation in local time between two adjacent satellites should roughly determine the limit on the scale size of the magnetospheric currents that can be resolved by this model.

4. Summary

We have presented an overview of the geosynchronous energetic electron response to the magnetic cloud event of January 10-11, 1997. This particular storm is the subject of much investigation because it is one of the first magnetic cloud events to be observed by the full complement of ISTP and supporting spacecraft. We have combined measurements from multiple spacecraft at geosynchronous orbit in order to develop a more comprehensive picture of the response of the magnetosphere to severe solar wind conditions. With five satellites simultaneously monitoring the geosynchronous environment we can produce a remarkably detailed picture of the magnetospheric response.

As one would expect, we found strong substorm-like activity associated with the passage of strong southward IMF B_z in the magnetic cloud. This activity included geosynchronous energetic particle injections, stretching and dipolarization of the magnetic field, and high levels of activity in the (preliminary) *AE*, Kp, and *Dst* indices. We call this activity "substorm-like" because individual substorms are nearly impossible to identify. Rather, the interval is characterized by nearly continuous, but sometimes localized, activity and by rapid fluctuations in the energetic particles and fields.

With the arrival of northward IMF the substorm-like activity at geosynchronous orbit and in the *AE* index abruptly ceased. However, the northward IMF was accompanied by a strong increase in the solar wind density, which compressed the magnetosphere and eventually pushed the magnetopause inside geosynchronous orbit. In combination with the earlier substorm activity this compression may have contributed substantially to the initial acceleration of relativistic electrons.

As we have shown, the geosynchronous relativistic electrons responded to the January 1997 magnetic cloud with two periods of enhanced fluxes. The first enhancement began when the IMF was still southward, near the time of minimum *Dst*, and prior to the peak compression of the magnetosphere. The initial enhancement lasted for approximately 24 hours with the highest flux levels of >2-MeV electrons measured between 1930 UT on January 10 and 0120 UT on January 11. This initial 1-day enhancement appears to be associated with the strong compression of the magnetosphere produced by the arrival of a density enhancement in the solar wind. The second enhancement was more gradual and delayed with peak fluxes observed on January 15.

Both electron flux enhancements can be understood if the initial source location for the >2-MeV electrons was located inside geosynchronous orbit on lower *L* shells. We postulate the following scenario. (1) Electrons are accelerated rapidly, within several hours of the arrival of the cloud, over a range of *L* shells,

with a peak in phase space density at a location $L<6.6$. (2) As the magnetic field becomes compressed, electrons with large pitch angles drift outward to conserve their first two adiabatic invariants. However, if the third invariant is not conserved, then the electrons can conserve energy. This transport produces the first electron flux peak, which is most intense near noon where the field is most compressed. (3) The most intense compression of the magnetosphere does not produce a further enhancement at geosynchronous orbit because the magnetopause is compressed inside that distance and dayside geosynchronous satellites are on extremely high L shells. (4) As the magnetospheric compression relaxes leading up to 1200 UT on January 11, the >2-MeV electrons again drift inward, and fluxes measured at geosynchronous orbit decrease. (5) Over the next several days the >2-MeV electrons can gradually diffuse outward to $L\approx6.6$ from the more stably trapped population at lower L shells, then peak and decay as the source population inside $L=6.6$ decays.

Steps 1 and 5 could be expected to occur in all relativistic electron events, while steps 2-4 would be expected only in particular circumstances. This scenario differs from the recirculation model in several important ways. It postulates an initial, rapid acceleration inside $L\approx6.6$. The acceleration can be impulsive rather than occurring over several days. It also accounts for more of the temporal structure and event-to-event variation seen at geosynchronous orbit. However, it also leaves the mechanism for the initial enhancement as an open question. We also note that while our proposed scenario is somewhat speculative it is consistent with the geosynchronous observations and can be tested by more extensive analysis using additional satellites.

In the second part of this paper we investigated the differences in geosynchronous relativistic electron fluxes measured simultaneously at different local times and introduced a data-based model of relativistic electron fluxes. We found that there were large differences in the fluxes throughout the period from January 10 to 18. During the second enhancement (e.g. January 12-18) the differences in the fluxes are well ordered with local time. Peak fluxes were measured near noon where the magnetic field is most dipole-like. Consistently lower fluxes were measured at midnight where the field is tail-like. Fluxes measured at dawn and dusk show a transition between higher fluxes on the dayside and lower fluxes on the nightside, but on average the dawn and dusk fluxes are comparable.

During the actual passage of the magnetic cloud on January 10 and 11 the differences in fluxes measured at various local times still followed the general trend of higher fluxes on the dayside and lower fluxes on the nightside but also showed other important variations. A comparison of the fluxes in 2-hour local time sectors at noon, midnight, dawn, and dusk shows that the relativistic electron fluxes rose first at noon and were followed by increases in the fluxes at dusk and then at dawn. A more complete synthesis for all local times shows that the dayside flux maximum moved around in local time and could be observed anywhere between dawn and dusk. Likewise, flux dropouts were observed on at least three occasions on January 10 and 11, each one in a different local time sector. The dropouts observed near midnight (0200 LT) and dusk (1900 LT) appear to have been caused by tail-like stretching of the magnetic field, which put the satellites on field lines that mapped to larger radial distances and hence lower energetic electron fluxes. The third dropout occurred around 1000-1100 LT and (as confirmed by MPA plasma data) was produced by a compression of the magnetosphere, which pushed the magnetopause inside geosynchronous orbit. Although this magnetopause compression might have been expected to produce a "drift shadow" leading to a loss of relativistic electrons, this effect was not observed and therefore might not typically play a significant role in the relativistic electron dropouts that are sometimes observed in the main phase of geomagnetic storms.

Within the last 10 years there has been a growing awareness of the importance of temporal changes in the energetic particle environment and especially the relativistic electron belts. Understanding those temporal variations is important both for basic magnetospheric physics and for the application that has come to be known as space weather. Space weather applications in particular will require development of global models that are driven in near real time by data from multiple satellites. The results of this study clearly show that, in addition to temporal and radial variations, local time variations must be included, and can be included, in those global models.

The January 1997 magnetic cloud-produced storm was not particularly unusual in terms of substorm activity, ring current strength, or relativistic electron fluxes. However, it provides an unusually good opportunity to exploit the potential of the International Solar Terrestrial Physics program and to develop tools and techniques for space weather applications. Understanding the complete Sun-Earth connection for this event will require understanding each of the components of the system and also the coupling between those components. The geosynchronous energetic particle environment is a particularly important, and interesting, piece in that larger puzzle.

Acknowledgments. This work was supported by NASA grant S19511E and by the Department of Energy Office of Basic Energy Science.

The Editor thanks M. Freeman and another referee for their assistance in evaluating this paper.

References

Acuna, M. H., K. W. Ogilvie, D. N. Baker, S. A. Curtis, D. H. Fairfield, and W. H. Mish, The global geospace science program and its investigations, in *The Global Geospace Mission*, edited by C. T. Russell, pp. 5-21, Kluwer Academic Publisher, Boston, 1995.

Baker, D. N., J. B. Blake, *L*. B. Callis, J. R. Cummings, D. Hovestadt, S. Kanekal, B. Klecker, R. A. Mewaldt, and R. Z. Zwickl, Relativistic electron acceleration and decay time scales in the inner and outer radiation belts: SAMPEX, *Geophys. Res. Lett., 21*, 409, 1994.

Baker, D. N., et al., An assessment of space environmental conditions during the recent Anik E1 spacecraft operational failure, *ISTP Newsl., 6, (2)*, 8, 1996.

Baker, D. N., T. Pulkkinen, X. Li, S. G. Kanekal, J. B. Blake, R. S. Selesnick, M. G. Henderson, G. D. Reeves, H. E. Spence, and G. Rostoker, Coronal mass ejections, magnetic clouds, and relativistic magnetospheric electron events: ISTP, *J. Geophys. Res.*, in press, 1998.

Baker, D. N., X. Li, J. B. Blake, and S. Kanekal, Strong electron acceleration in the Earth's magnetosphere, Adv. Space Sci., in press, 1998*b*.

Belian, R. D., G. R. Gisler, T. E. Cayton, and R. Christensen, High *Z* energetic particles at geosynchronous orbit during the great solar proton event of October, 1989, *J. Geophys. Res., 97*, 16,897, 1992.

Blake, J. B., et al., Correlation of changes in the outer-zone relativistic electron population with upstream solar wind and magnetic field measurements, *Geophys. Res. Lett., 24*, 927-929, 1997.

Bothmer, V., and R. Schwenn, The interplanetary and solar causes of major geomagnetic storms, *J. Geomagn. Geoelectr., 47*, 1127-1132, 1995.

Friedel, R. H. W., and A. Korth, Long-term observations of keV ion and electron variability in the outer radiation belt from CRRES, *Geophys. Res. Lett., 22*, 1853, 1995.

Li, X., D. N. Baker, M. Temerin, T. E. Cayton, E. G. D. Reeves, R. A. Christensen, J. B. Blake, R. Nakamura, and S. G. Kanekal, Multi-satellite observations of the outer zone electron variation during the Nov. 3-4, 1993 magnetic storm, *J. Geophys. Res., 102*, 14,123, 1997.

Meier, M. M., R. D. Belian, T. E. Cayton, R. A. Christensen, B. Garcia, K. M. Grace, J. C. Ingraham, J. G. Laros, and G. D. Reeves, The energy spectrometer for particles (ESP): Instrument description and orbital performance, in *Workshop on the Earth's Trapped Particle Environment*, edited by G. D. Reeves, pp. 203-210, AIP Press, New York, 1996.

Office of the Federal Coordinator for Meteorology, National Space Weather Program: Implementation Plan, Publ. *FCM-P31-1997*, Washington, D. C., 1997.

Paulikas, G. A., and J. B. Blake, Effects of the solar wind on magnetospheric dynamics: Energetic electrons at the synchronous orbit, in *Quantitative Modeling of Magnetospheric Processes, Geophys. Monogr. Ser.*, vol. 21, edited by W. P. Olson, p. 180, AGU, Washington, D. C., 1979.

Wrenn, G. *L*., Conclusive evidence for internal dielectric charging anomalies on geosynchronous communications spacecraft, *J. Spacecr. Rockets, 32*, 514-520, 1995.

D. N. Baker and X. Li, Laboratory for Atmospheric and Space Physics, University of Colorado, Boulder, CO 80302. (e-mail: baker@orion.colorado.edu; lix@kitron.colorado.edu)

R. D. Belian, R. H. W. Friedel, M. G. Henderson, M. M. Meier, and G. D. Reeves, Los Alamos National Laboratory, Los Alamos, NM 87545. (e-mail: rdbelian@lanl.gov; rfriedel@lanl.gov; mghenderson@lanl.gov; mmeier@lanl.gov; reeves@lanl.gov;)

J. B. Blake, The Aerospace Corporation, Los Angeles, CA 90009. (e-mail: blake@dirac2.dnet.nasa.gov)

T. ONSAGER AND H. J. SINGER, NOAA SPACE ENVIRONMENT CENTER, BOULDER, CO 80303. (E-MAIL: TONSAGER@SEC.NOAA.GOV; HSINGER@SEC.NOAA.GOV)

Table 1. Geosynchronous Satellite Positions.

Satellite	Longitude	Local Time
1990-095	-37.4	LT≈UT-2.5
1991-080	70.8°	LT≈UT+4.7
1994-084	103.8°	LT≈UT+6.9
GOES 8	-74.7°	LT≈UT-5.0
GOES 9	-135.1°	LT≈UT-9.0

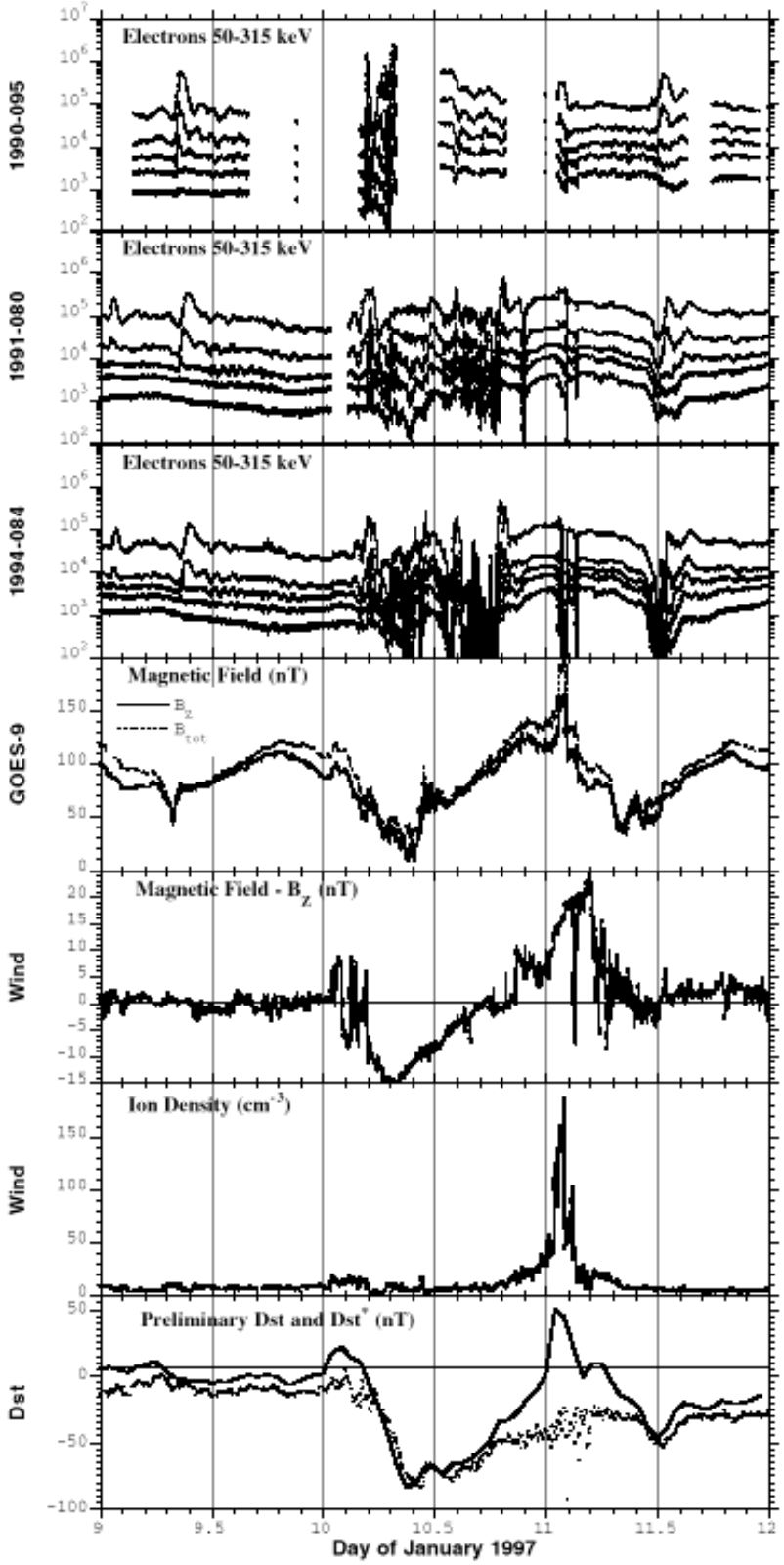

Figure 1. Overview of magnetospheric and solar wind conditions on January 9-12. The top three panels show LANL geosynchronous energetic electron data (50-315 keV). The next panel shows GOES 9 magnetic field data. The next two panels show the *Z* component of the IMF and the solar wind ion density. The bottom panel shows the preliminary *Dst* index as a solid line and the pressure-corrected *Dst** as dots. As we discussed in the text, the figure illustrates the magnetospheric response to the strong southward IMF conditions and to the northward IMF and magnetospheric compression that followed.

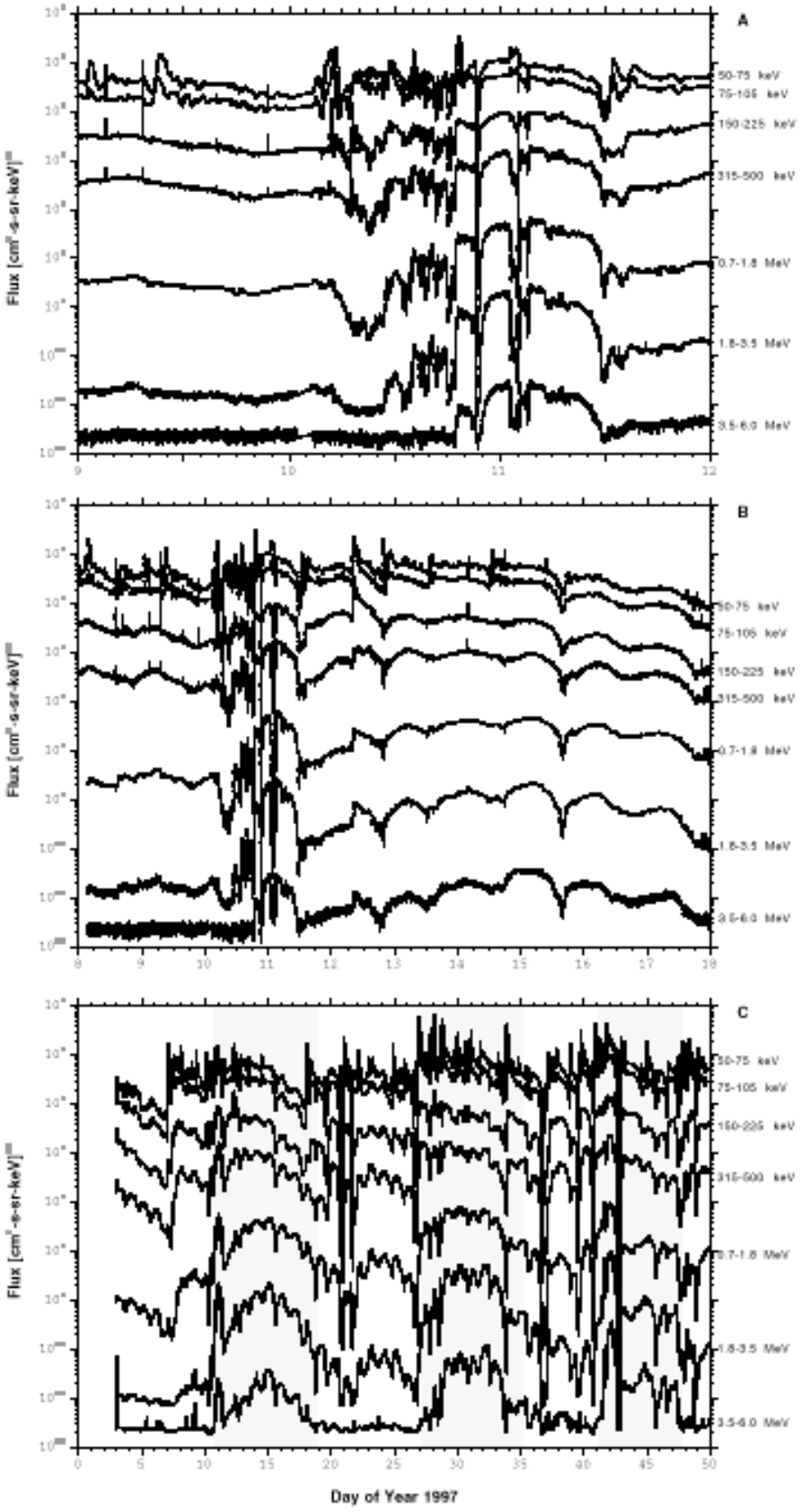

Figure 2. Energetic electron response measured by spacecraft 1991-080 from 50 keV to 6 MeV on (a) January 9-12, (b) January 8-18, and (c) days 3-50. Figure 2a shows the initial response to the passage of the magnetic cloud. Figure 2b additionally shows a secondary but delayed enhancement of the relativistic electrons. Comparison with Figure 2c shows that the January 10, 1997 event was not exceptional in terms of substorm activity or in terms of the magnitude or duration of the relativistic electron enhancement.

Reeves et al., JGR, 1998

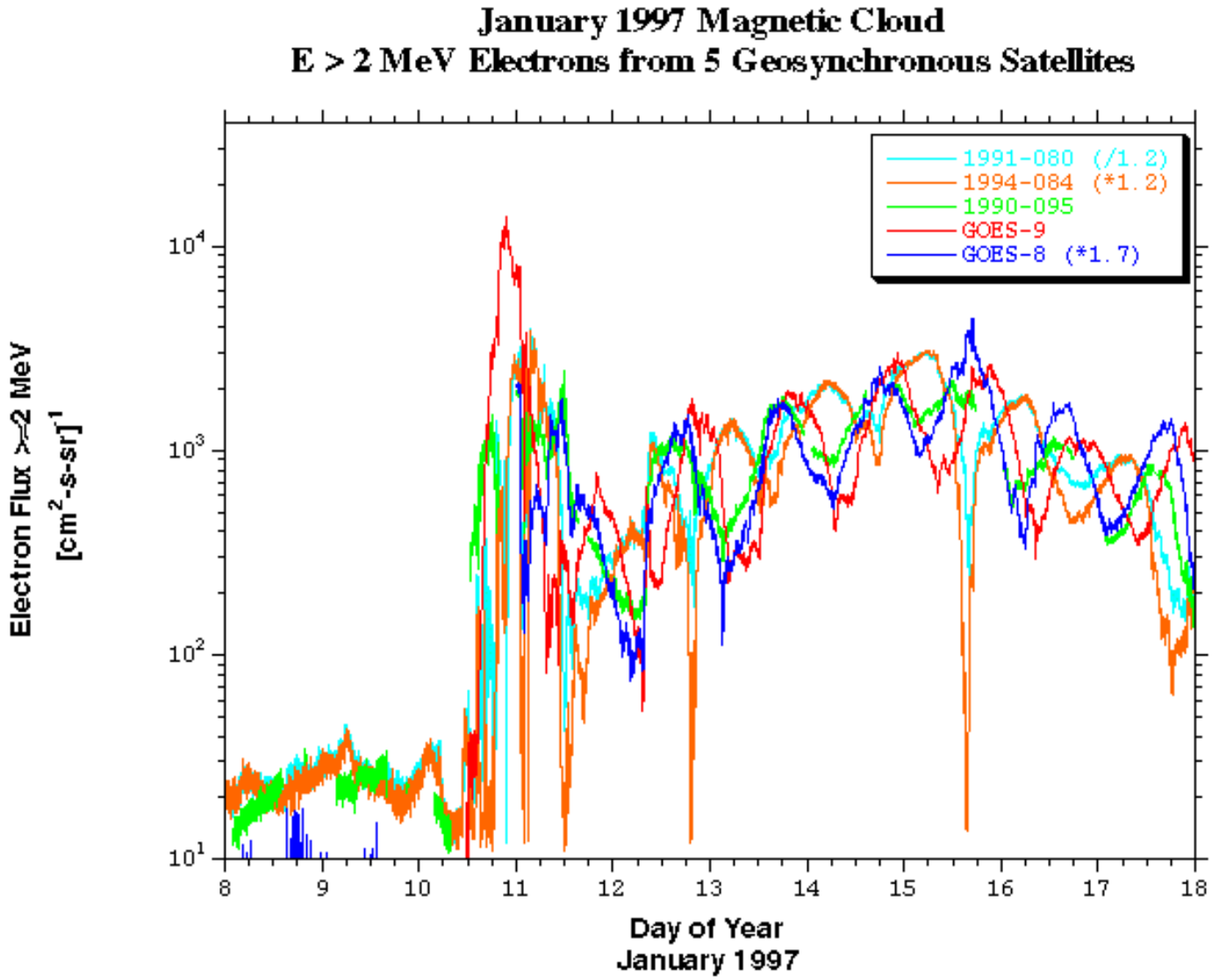

Plate 1. Data from five geosynchronous satellites for energies of approximately >2 MeV. The fluxes have been normalized so the dayside peaks measured on January 12-18 are roughly equal.

Reeves et al., JGR, 1998

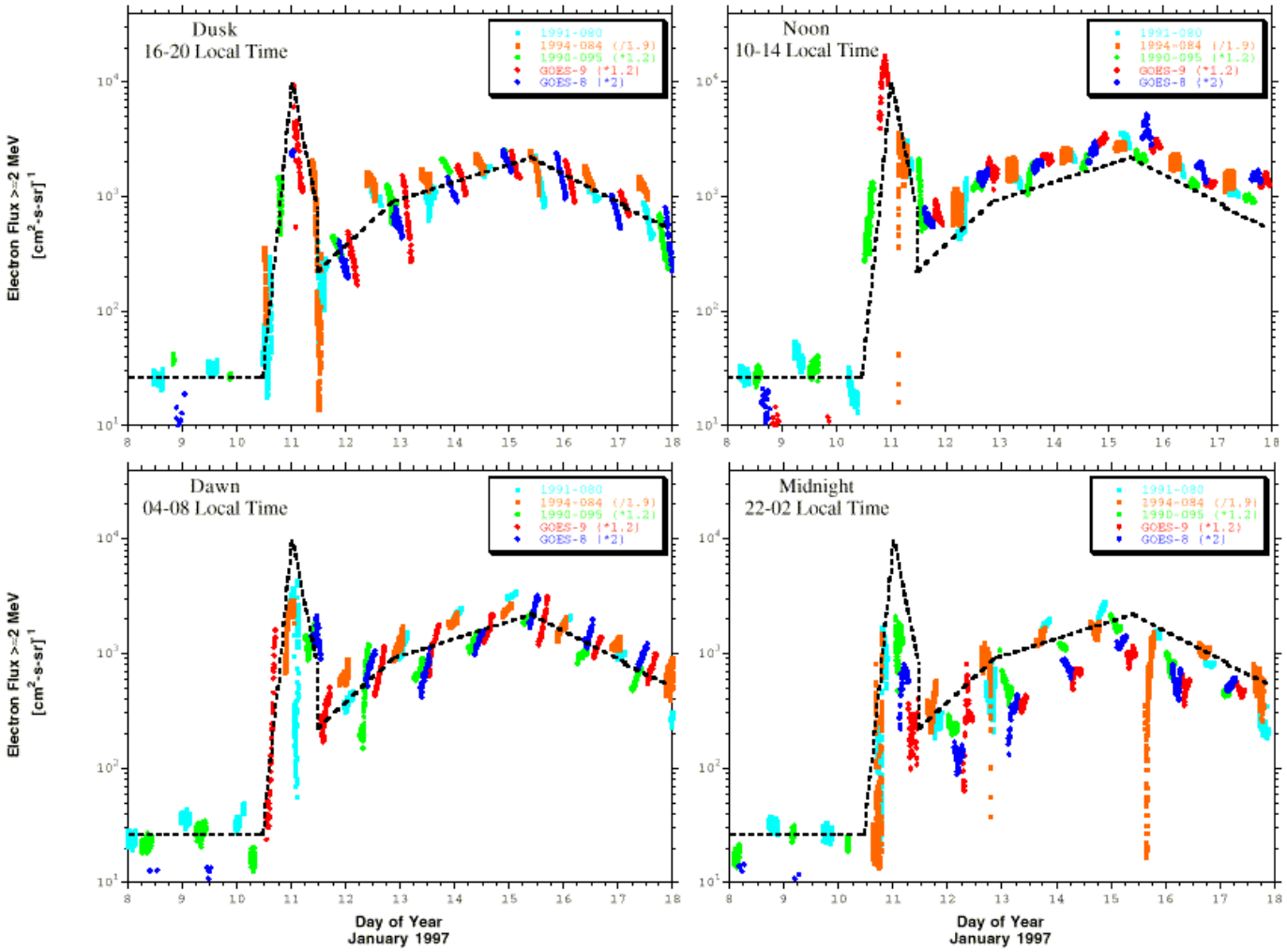

Plate 2. The >2-MeV electron response in four local time sectors. Data from all five geosynchronous satellites are plotted in 4-hour local time sectors centered on dusk, dawn, noon, and midnight. A common reference curve is also plotted. The variations in local time are primarily produced by the asymmetry of the magnetospheric magnetic field.

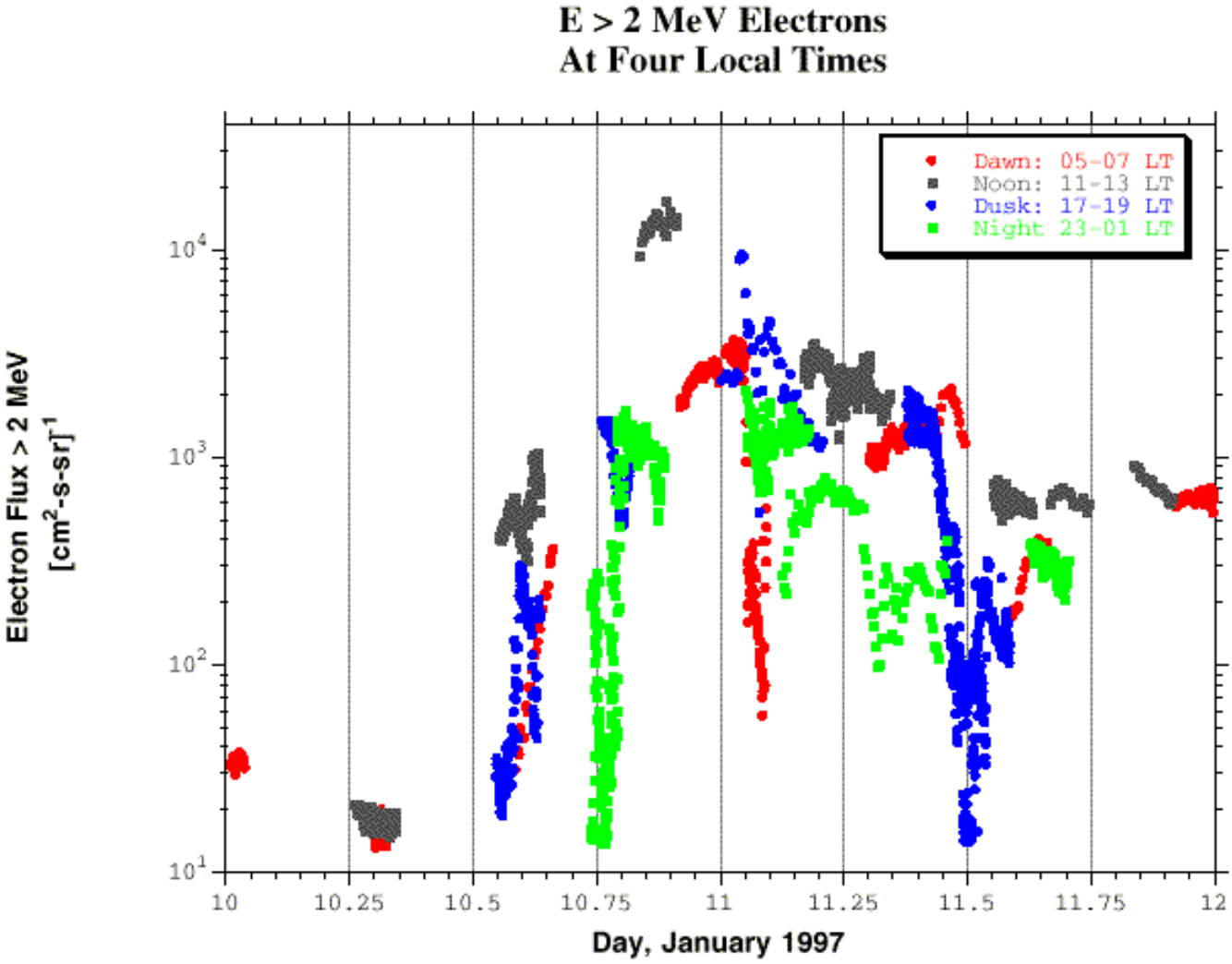

Plate 3. Data from all five geosynchronous satellites shown in high time resolution for 2-hour bins centered at dawn, noon, dusk, and midnight. Large differences in the fluxes measured simultaneously at different local times can be seen. During this highly disturbed period the differences are not well ordered by noon-midnight asymmetries.

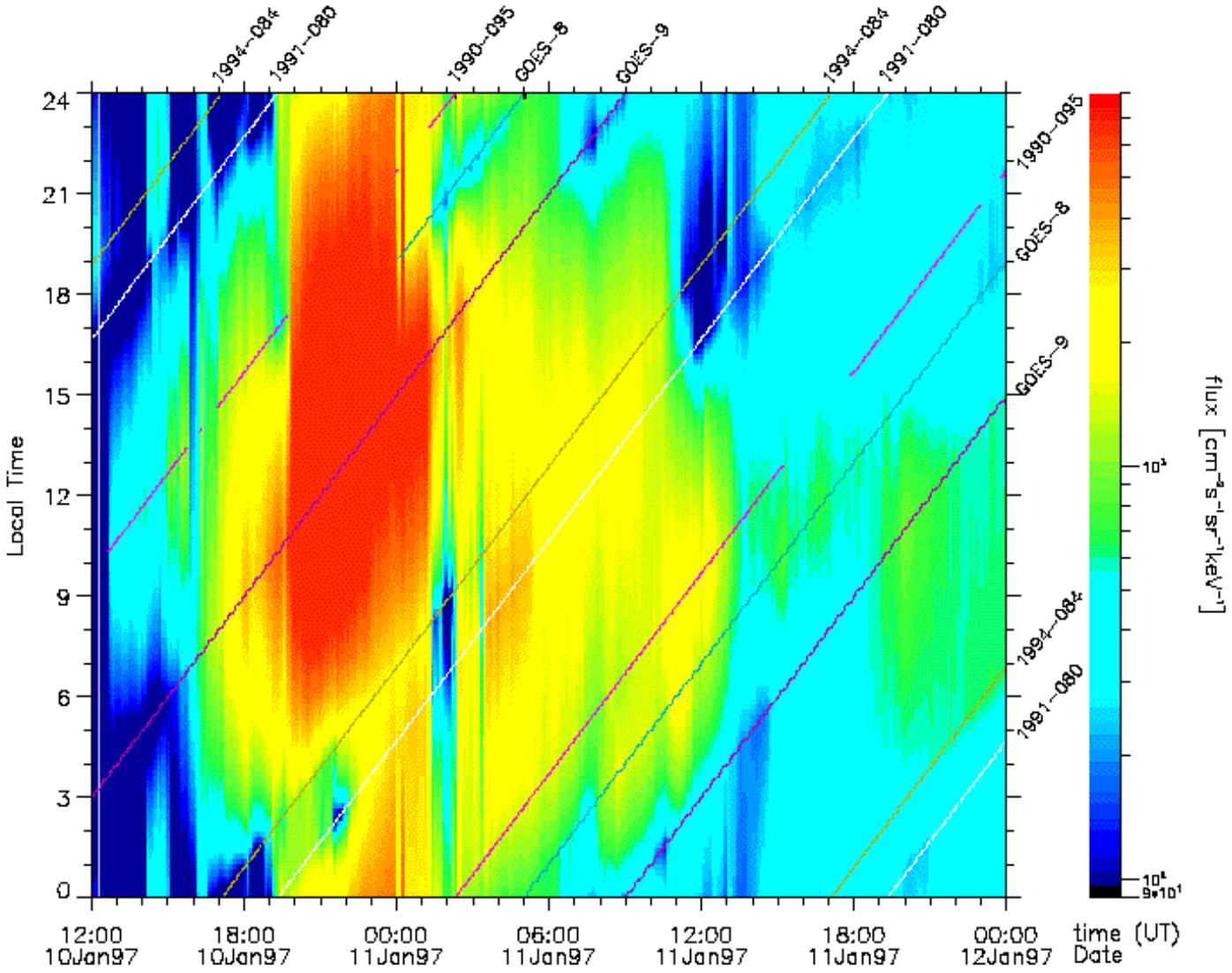

Plate 4. Data-driven synthesis model of the >2-MeV electron fluxes at geosynchronous orbit. Flux is color coded and plotted as a function of local time and universal time. The satellite tracks in this coordinate system appear as diagonal lines. Flux values between satellite positions are interpolated. The large variation in fluxes measured simultaneously at different local times is apparent. Both peak flux regions (red) and dropout regions (dark blue) are seen to vary in local time.

Author's Note: Because of the large size of the electronic files for some of these figures they are provided here as bit-mapped images. Postscript and Adobe Acrobat versions of all the figures are available by request to Geoff Reeves, Mail Stop D-436, Los Alamos National Lab., Los Alamos, NM 87545; phone 505-665-3877; e-mail REEVES@LANL.GOV.